

Magnetism of Fe clusters embedded in a Co matrix from first-principles theoryAnders Bergman,^{1,*} Erik Holmström,¹ A. M. N. Niklasson,² Lars Nordström,¹ Sonia Frota-Pessôa,³ and Olle Eriksson¹¹*Department of Physics, Uppsala University, Box 530, S-751 21 Uppsala, Sweden*²*Theoretical Division, Los Alamos National Laboratory, Los Alamos, New Mexico 87545, USA*³*Instituto de Física, Universidade de São Paulo, Caixa Postal 66318, 05315-970, São Paulo, SP, Brazil*

(Received 17 June 2004; revised manuscript received 20 September 2004; published 22 November 2004)

We have calculated spin and orbital moments for Fe clusters of sizes up to 700 atoms embedded as impurities in a bcc Co matrix. The calculations have been carried out using relativistic first-principles real-space density functional theory, and we have made a comparison with earlier experimental studies. For Fe atoms close to the Fe—Co interface, the spin moments are found to increase while atoms far from the interface exhibit bulklike moments. The Co moments remain essentially unchanged and close to the moment of bulk bcc Co. With increasing cluster size, the average moments of the cluster atoms decrease due to the decreased surface to volume ratio. The orbital moments of both Fe and Co are calculated to be small and they stay almost constant regardless of cluster size. Our results for spin moments agree with experimental data but the calculated orbital moments are slightly underestimated. A simplified model indicates that a compound of close-packed Fe clusters surrounded by Co show higher average total moments compared to bulk and multilayer systems with a similar concentration. This increase seems to disappear when cluster-cluster interactions are taken into account. The general trend is that for a given alloy concentration of $\text{Fe}_x\text{Co}_{1-x}$, clustering tends to lower the average magnetic moment compared to that of ordered structures and random alloys.

DOI: 10.1103/PhysRevB.70.174446

PACS number(s): 75.75.+a, 71.15.Mb, 73.22.-f

I. INTRODUCTION

Magnetic nanoscale clusters of transition metals have recently attracted much attention since such clusters may have novel properties that are different from bulk, multilayer, or molecular systems. The progress of improving depositing techniques with increasing accuracy of size distributions and characterization of clusters¹ has also made it easier to compare well-defined systems with calculations. One system that shows interesting behavior and that has been thoroughly examined is Fe clusters. Stern-Gerlach experiments of free Fe clusters by Billas *et al.*^{2,3} have shown increased magnetic moments for small clusters with an oscillating decrease towards the bulk value for large cluster sizes. Theoretical work on similar free Fe clusters has examined the magnetic properties⁴⁻⁶ as well as equilibrium structures.⁷⁻⁹

Improved techniques for producing clusters with well-controlled size distributions, and methods of depositing clusters while embedding them in another material, have increased the research activity in this field,^{10,11} which has paved the way for creating cluster-based materials with tailored compositions and properties. Many of these novel properties from embedded clusters are interesting for applications. Examples of this are granules of Co that in a non-magnetic matrix are known to exhibit giant magnetoresistance^{12,13} (GMR) and Co clusters embedded in insulating matrices that have shown large tunneling magnetoresistance¹⁴ (TMR). Theoretical work on binary systems with Fe clusters has mostly been done for adatoms or clusters on surfaces¹⁵⁻¹⁸ while studies of embedded clusters are more limited.¹⁹⁻²¹

Fe clusters in Co are interesting for applications where a high magnetization density is desirable. The reason is the analogy with Fe—Co alloys that might cause interesting behavior. Body-centered-cubic Fe—Co alloys show a nonlinear concentration dependence of the magnetic moment. As

polarized neutron diffraction²² studies show, this behavior is due to an increase of the Fe spin moment for an increasing Co concentration. The spin moment of Fe increases from the bulk value to a maximum of $\sim 3\mu_B$ /atom for 50% Co. The Co moment stays nearly constant over the whole concentration range. The average magnetic moment follows the Slater-Pauling curve²³ with a maximum magnetic moment of $\sim 2.45\mu_B$ /atom for a concentration of $\sim 30\%$ Co. This peak also gives the highest known saturation field for bulk materials with a value of ~ 2.45 T. In many applications it is desirable to increase this number. One way to break this current limitation and to increase the saturation magnetization might be to use tailored systems that behave differently from bulk materials, such as multilayers and cluster-based materials.

In this paper we study the magnetic behavior of Fe clusters within the size range of 1–701 atoms embedded in Co. Such systems seem promising for producing materials with high saturation magnetization, and have been extensively examined experimentally. Baker *et al.*,²⁴ Binns *et al.*,²⁵ and Edmonds *et al.*²⁶ have performed x-ray magnetic circular dichroism (XMCD) measurements on exposed and Co-coated Fe clusters and have noticed an increase in the spin moment and an even larger relative enhancement of the orbital moments in comparison with bulk Fe. Despite intense experimental efforts, theoretical works on embedded Fe clusters in Co are essentially lacking. Some calculations have, however, been published, e.g., by Xie and Blackman,¹⁹ who based their calculations on a parametrized tight-binding method that neglects spin-orbit coupling. The present work is based on a parameter-free, fully relativistic, self-consistent real-space linear muffin-tin orbital atomic-sphere approximation (RS-LMTO-ASA) technique that can calculate spin and orbital moments for different sizes of Fe clusters embedded in Co in a highly accurate way.

II. THEORY

The RS-LMTO-ASA technique²⁷ is a self-consistent method that is similar to the ordinary k -space LMTO-ASA method,^{28,29} except that the eigenvalue problem is solved by means of the recursion method.³⁰ It is a method that is well suited for complex systems without periodicity since the computational effort scales linearly with the number of inequivalent atoms and has been successfully applied to studies of impurities and other defects in metals³¹ and also on metallic surfaces. It has recently been used for calculations on Fe—Co multilayers as well.³² The LMTO-ASA method is a linear method with solutions accurate around a linearization energy E_ν , usually taken at the center of the occupied part of the bands. Starting from the orthogonal representation of the LMTO-ASA formalism, where the overlap matrix is approximated as the unity matrix, an expansion that is accurate to $(E-E_\nu)^2$ can be constructed. In this scheme, the Hamiltonian can then be expressed in terms of potential parameters from the tight-binding representation of LMTO-ASA as

$$H = E_\nu + \bar{h} - \bar{h}\bar{o}\bar{h} \quad (1)$$

with

$$\bar{h} = \bar{C} - E_\nu + \bar{\Delta}\bar{S}\bar{\Delta}. \quad (2)$$

Here \bar{C} , \bar{o} , and $\bar{\Delta}$ are potential parameters and \bar{S} is the structure matrix in the tight-binding LMTO-ASA representation. These potential parameters are related to the solutions of the Schrödinger-like equation inside the atomic spheres around each site, and are determined self-consistently. The spin-orbit interaction is treated at each variational step. This method of including spin-orbit effects is known to give very similar results to calculations based on the Dirac equation, both in terms of details in the electronic structure as well as spin and orbital moments. For instance, the spin and orbital moment of Fe, Co, and Ni were in Ref. 34 calculated with a Dirac LMTO-ASA method and they agree within a few percent to the calculation in Ref. 35 that used a similar method for treating relativity as we do here. In addition, orbital polarization³³ is included.

Since the Fe clusters in this study are embedded in Co, they are treated as a local perturbation to the surrounding host, where Co atoms far from the cluster have fixed potential parameters of bulk bcc Co, while Co atoms closer to the Fe cluster are treated self-consistently. Charge transfer between the self-consistent region and the surrounding bulk is taken care of by integrating the density of states up to the Fermi level of the surrounding bulk Co and then distributing the excess charge from the perturbation to the nearest bulk neighbors.²⁷

The Co atoms that have been treated self-consistently have potential parameters that are almost identical to the potential parameters of bulk Co. The charge transfer between Fe and Co atoms is also small for these systems. This allows us to make the approximation that the calculated properties of the Fe atoms do not depend on whether the surrounding Co atoms are treated self-consistently or not. We have tested this approximation for a cluster of 51 atoms and found that it

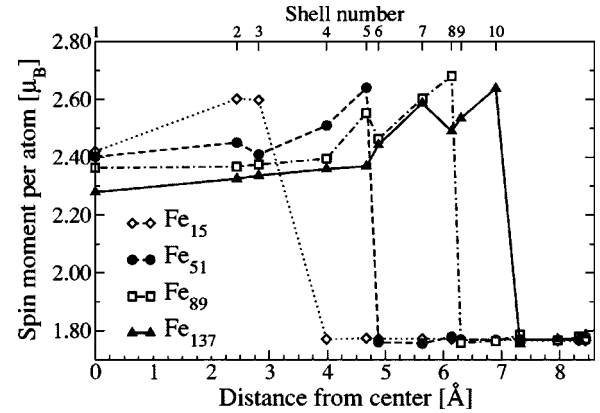


FIG. 1. Local spin moment per atom for each shell for different cluster sizes. The calculated individual Fe moments increase up to $\sim 2.6\mu_B/\text{atom}$ for atoms close to the Fe—Co interface. The Co atoms have almost constant moments of about $\sim 1.75\mu_B/\text{atom}$.

is accurate, with an error of less than $\sim 1\%$, and we have used this approximation for the Fe clusters that are larger than 150 atoms.

The continued fraction in the recursion method is terminated after 30 recursion steps with the Beer-Pettifor terminator.³⁶ To simulate the surrounding bulk, more than 15 000 Co atoms surrounding the Fe cluster are used. Finally, we have used the von Barth—Hedin exchange-correlation functional within the local spin-density approximation (LSDA).³⁷

III. RESULTS

A. Cluster impurities

The thickness of the covering Co layers on the Fe clusters in the previously mentioned studies^{24–26} was estimated to be 10 Å and thus we find it reasonable to treat the Fe clusters as fully embedded in Co. For small Fe clusters, the crystal structure is not fully known, but the bcc structure is generally assumed. Since Co is known to be stabilized in the bcc structure in thin Fe—Co multilayers, we have assumed a bcc structure both for the Fe clusters and the surrounding Co matrix. In our study, we have considered clusters with a spherical growth pattern. This can be viewed as the clusters having an onionlike structure, consisting of an increasing number of shells of equivalent atoms. For large clusters, this may be a severe approximation since the clusters would minimize their surface energy and consequently have large areas of principal surfaces.³⁸ However, the studied clusters in this article are of limited size and then this effect is weak due to the small surface area. In most of the calculations we have used the experimental lattice parameter for bcc Fe. For some calculations we have also compared with results given for a lattice parameter corresponding to that of bcc Co when extrapolating the experimental lattice parameter for bcc Fe—Co alloys to the limit of pure Co.³⁹ This parameter is less than 2% smaller than the lattice parameter of pure Fe.

In Fig. 1 we show the local atomic spin moment per atom for each shell of the clusters. The central Fe atom of each

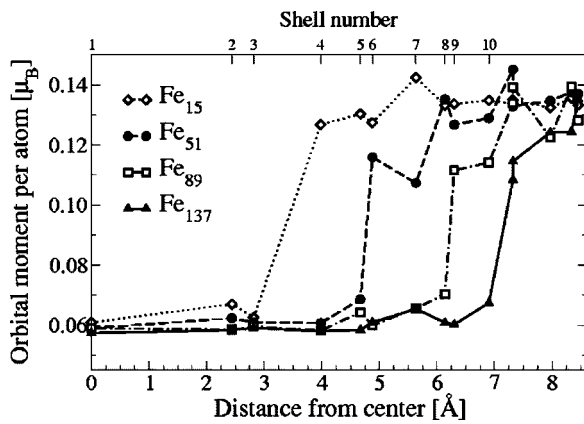


FIG. 2. Local orbital moment per atom for each shell for different cluster sizes. The calculated orbital moments on the Fe atoms are constant at around $0.06\mu_B/\text{atom}$. The Co atoms have a higher orbital moment that decreases slightly close to the Fe—Co interface.

cluster is located at zero on the x axis. For every cluster size the local magnetic moment per shell is then plotted. For instance, the Fe_{15} cluster consists of three shells of Fe atoms and from the fourth shell on there are only Co atoms. For this cluster, the outermost Fe shell has a local spin moment of $\sim 2.6\mu_B/\text{atom}$ and the neighboring Co shell has a moment of $\sim 1.75\mu_B/\text{atom}$. In all calculations we find that the spin moments of the Co atoms are essentially insensitive to the number of surrounding Fe atoms. In every curve in Fig. 1 the “step” in the magnetic moment characterizes the transition from Fe shells to Co shells.

In general, when moving outwards shell by shell from the center of a cluster, the number of neighboring crystallographic sites that are occupied by Co atoms increases. Assuming dominating nearest-neighbor interactions, the shape of, e.g., the Fe_{137} result (Fig. 1) can then be interpreted as follows: An atom in shell 5 and below has no Co atoms as nearest neighbors and in this region the magnetic moment changes slowly with distance from the center of the cluster. From shell 6 and above the number of nearest neighbors that are Co atoms is increasing and the local Fe moment hence increases quite dramatically. Our interpretation of this result is that the spin moment of Fe is enhanced by the proximity to the Co atoms. This analysis is consistent with what is known from bulk alloys, surfaces, and interfaces.^{40–42} The effect is not long range but seems to be limited to nearest neighbors. In addition to the interface effect, quantum-well effects originating from multiple scattering at the cluster boundaries may affect the magnetic moments. However, our calculated magnetic moment on the central atom in the clusters does not show oscillatory behavior for different cluster sizes as would be expected from such interference effects.

In Fig. 2 we show the calculated orbital moments for the same systems as in Fig. 1. We find that the trend is different from the spin moments since now the Fe moments are almost constant and low, whereas the Co moments show a small decrease in the proximity of the Fe atoms. For both types of atoms we see only a small effect on the orbital moments from the number of foreign nearest neighbors. Our calculated

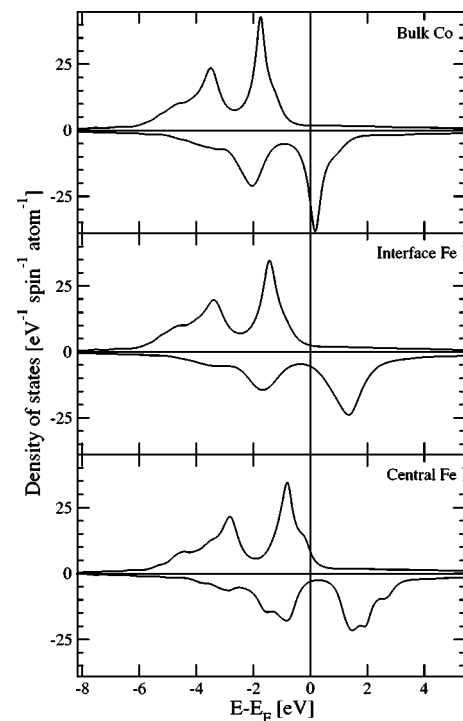


FIG. 3. Local density of states (LDOS) for atoms in a Fe_{137} cluster. The LDOS shown are for a Co atom in the bulk region, an Fe atom at the interface and an Fe atom in the center of the cluster. The density of states for the Co atoms at the interface is almost identical to that for bulk Co atoms and are therefore not displayed. The Fermi level is at zero energy and is given as a vertical line.

orbital moments for the Co atoms are approximately $0.14\mu_B/\text{atom}$ whereas the orbital moment of the Fe atoms are of the order of $0.06\mu_B/\text{atom}$, regardless of the position of the atom in the cluster. The latter number is lower than the experimental value for similar systems, since values around $0.15\mu_B$ have been reported.²⁵ However, our calculated values are in quite good agreement with the bulk value of bcc Fe, $0.08\mu_B/\text{atom}$.

The reason why the experimental values of the clusters are larger than theory may be explained either from difficulties in determining orbital moments via the XMCD sum rules, or due to the fact that there might be relaxation effects in the experimental clusters. These relaxations lower the symmetry and change the coordination for the Fe atoms, which therefore might increase the orbital moments.

We now turn our attention to the mechanism why the spin moments of bcc Fe are enhanced at the interface with Co, and for this reason we display in Fig. 3 the local density of states (DOS) of selected cluster atoms. As can be seen in Fig. 3 the Fe atom in the center of the cluster has a DOS that is very similar to bulk bcc Fe. However, although the Fe atom at the interface with Co has similar features as the Fe atom at the center of the cluster, there is a marked difference in that the band filling is much higher. In particular, one encounters a situation where the spin up band of the interface Fe is full, a situation normally referred to as “strong” ferromagnetism. Since there is very little charge transfer between any atom in the cluster (there is a small charge transfer of 0.05 electrons from the interface Fe atom to Co), this means that the inter-

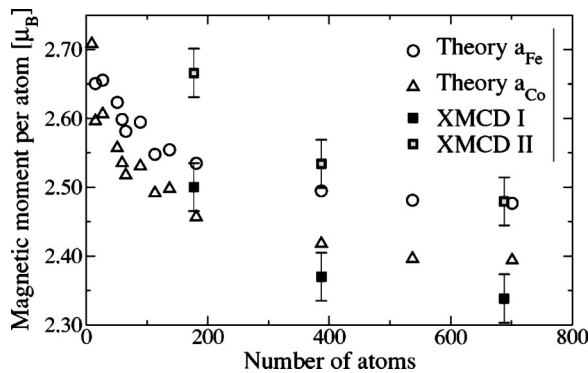


FIG. 4. Averaged total moments for the Fe atoms as a function of number of cluster atoms. The black squares represent experimental (XMCD) data (Ref. 25) and gray squares represent another set of XMCD data (Ref. 44), corrected for a systematic error. Open circles represent theoretical calculations with the bcc Fe lattice parameter and open triangles theoretical values with the bcc Co lattice parameter.

face Fe atom has transferred some of its spin-down electrons to spin-up electrons, with an increased spin moment as a result. It may even be observed in Fig. 3 that the most conspicuous peaks of especially the spin-up band of the interface Fe atoms are almost coinciding with the corresponding peaks of the interface Co atom, a result of strong hybridization between these two atoms. We end this paragraph by noting that a full analysis of these effects may be found in the textbook of Mohn.⁴³

In Fig. 4 we show the average Fe magnetic moment of each cluster, i.e., the sum of the spin and orbital moments divided by the number of Fe atoms in a cluster. Experimental data from Binns *et al.*^{25,44} are also shown. The average Fe magnetic moment is decreasing when the cluster size becomes larger both in the calculations and in the experiments. We interpret this as a result of a smaller surface to volume ratio for the larger clusters, and since the enhanced Fe moments are located in the surface region, the average moment decreases. In the limit of large clusters one thus expects the average moment to approach the bulk moment of bcc Fe asymptotically as $1/R$, where R is the radius of the cluster.

When comparing our calculations with the previously mentioned experiments, it is worth pointing out that even though the mass for these clusters is well defined, the shapes and lattice parameters of the clusters are not known. The crystallographic structure is not fully known either but at least the inner parts of the clusters are expected to have a bulklike bcc structure. There might also be some alloying present in the Fe—Co interfaces present in the experiments that is neglected in the calculations. Nevertheless, our calculated total moments agree with the trend of the experimental data. As regards a quantitative comparison one must first note that in Fig. 4 we show two sets of experimental values: one is from a direct measurement²⁵ using XMCD, which unfortunately gives somewhat too low a moment for bulk bcc Fe. For this reason a smaller correction was made in a second experiment⁴⁴ also based on the XMCD technique. This correction amounted to a small moment ($0.17\mu_B/\text{atom}$) being added to the measured Fe spin moments of all clusters.

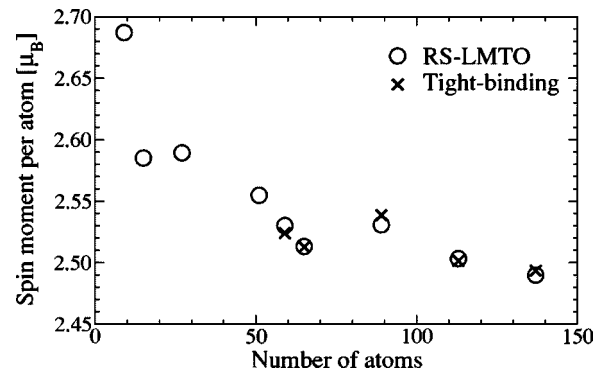


FIG. 5. Averaged local spin moments of Fe atoms as a function of cluster size. The nonmonotonic decrease is due to different coordination for the Fe atoms. Comparison is made with parametrized tight-binding calculations (Ref. 19).

As is clear from Fig. 4, theory and experiment agree very well for larger Fe clusters. The corrected experimental values are approaching asymptotically the bulk value of bcc Fe (slightly larger than $2.2\mu_B/\text{atom}$), whereas the theoretical value approaches a somewhat larger bulk moment of $2.3\mu_B/\text{atom}$. This small discrepancy between theory and experiment is well known for LSDA (and generalized gradient approximation) based theories.⁴³ For smaller clusters theory underestimates the (corrected) experimental values with $\sim 0.1\mu_B/\text{atom}$. Hence we draw the conclusion that the present calculation reproduces the measured moments with an error not exceeding 5%, and that theory sometimes underestimates the moment (smaller clusters) and sometimes overestimates the moment (bulk values). In order to investigate the effect on volume we performed additional calculations using the Co Wigner-Seitz radius. As is clear from Fig. 4 this influences the total moment only to a small degree.

Since interface atoms have a higher moment than bulk atoms and generally the ratio between interface and bulk atoms decreases with increasing cluster size, an increase of the cluster size generally lowers the total magnetic moment. But for the small clusters we find that this trend is not always true. The number of Fe atoms with many Co neighbors varies for these small clusters, so that the decreasing trend is not entirely monotonic. For instance, an Fe cluster consisting of 65 Fe atoms has 14 Fe atoms with 4 Co neighbors each, while an 89-atom Fe cluster has 24 Fe atoms with 6 Co neighbors, thus the average moment is higher for the larger cluster. This can be seen in Fig. 5 where we compare our calculated spin moments with previous parametrized calculations.¹⁹ Both types of calculations give similar values and the same trend.

B. Cluster-based alloys

Since Fe clusters show high total moments, it is reasonable to assume that a cluster-based Fe—Co alloy may exhibit high saturation magnetization. As is seen from our calculations, the most important factor for enhancing the magnetic moment of the Fe clusters is to maximize the number of Co neighbors for the Fe atoms. But since the Co atoms have an almost constant magnetic moment, that is lower than

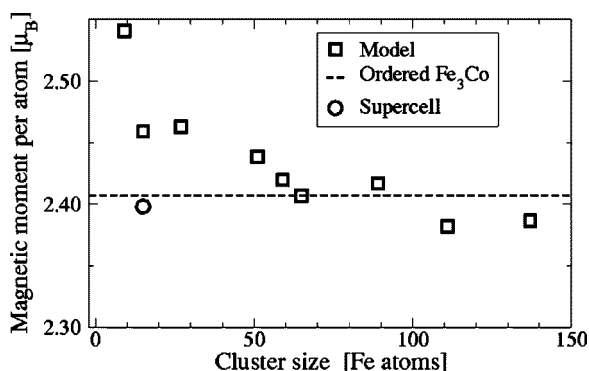


FIG. 6. Theoretical data of the average total magnetic moment for various Fe—Co systems with 25% Co concentration. The squares represents Fe clusters covered with Co. The dashed line refers to ordered Fe₃Co (*D0*₃) bulk alloy. The result from a supercell calculation simulating close-packed Fe₁₅ clusters surrounded by ~25% Co is also shown. For this packed structure, the average moment is decreased due to cluster-cluster interactions.

the Fe moment, an increased number of Co atoms in the material tends to decrease the total magnetization density. Hence, the key to high saturation magnetization density is to minimize the amount of Co atoms while maximizing the number of Co neighbors for the Fe clusters. The number of Co atoms needed to fill out the voids between clusters can be minimized if the Fe clusters are packed as close together as possible in the Co matrix.

1. Noninteracting clusters

A simple model of a material built up by Fe clusters surrounded by Co can be constructed in the following way. If the Fe clusters are considered as spherical and of the same size, then the number of Co atoms filling out the interstitial region can be minimized to a concentration of about 25%, by close packing the clusters. By using this geometry and also assuming that the Fe clusters do not interact with each other, our results for the magnetic moments of Fe clusters can be used to estimate the average magnetization density for such cluster-based materials.

With this geometry, the average moment of the cluster-based material can then be calculated by taking the average moment over not only the Fe clusters, but also a number of surrounding Co atoms, corresponding to 25% of the total number of atoms. In Fig. 6 we investigate the total magnetic moment of such hypothetical materials that are based on close-packed monodisperse Fe clusters.

As can be seen in Fig. 6, the moments are decreasing with increasing cluster size. This indicates that large clustering effects in an Fe—Co alloy tend to lower the total magnetic moment. In Fig. 6, the moment for an ordered Fe₃Co (*D0*₃) bulk alloy is also plotted. Since this alloy lies almost at the peak of the Slater-Pauling curve, the magnetic moment of this compound is a good reference value. According to Fig. 6, materials based on clusters larger than ~50 atoms will not have higher saturation magnetization than an ordinary Fe—Co alloy. However, alloys with clusters containing less than ~50 Fe atoms could, in this model, yield a higher moment than the Slater-Pauling curve predicts.

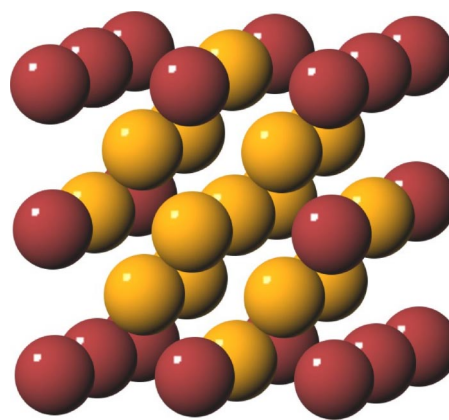


FIG. 7. (Color online) The supercell used in the calculations for packed Fe₁₅ clusters embedded in 25% Co. For this low concentration, neighboring clusters are sharing their outmost Fe atoms.

2. Interacting clusters

In the noninteracting cluster model mentioned above, the total moment for smaller clusters at low Co concentrations is higher than that for bulk alloys, suggesting that high moment materials might be built from such systems. However, it might be difficult to retain these high moments achieved within our simplified model, since for the low Co concentration that is necessary to keep the average moment high enough, the Fe clusters will not have the same coordination of Co neighbors as in the model case. The clusters will have more Fe neighbors instead, which results in interactions between the Fe atoms in neighboring clusters and a possible decrease of the moments. To investigate this, we have performed a supercell calculation within the RS-LMTO scheme. The supercell system consists of packed Fe₁₅ clusters with a global Co concentration of 25%, as displayed in Fig. 7. The clusters were aligned ferromagnetically and no other magnetic ordering was considered, since the clusters are close enough to each other to share Fe atoms.

The magnetic moment for each shell for the Fe₁₅ single-impurity cluster and the packed, fully interacting, Fe₁₅ super-

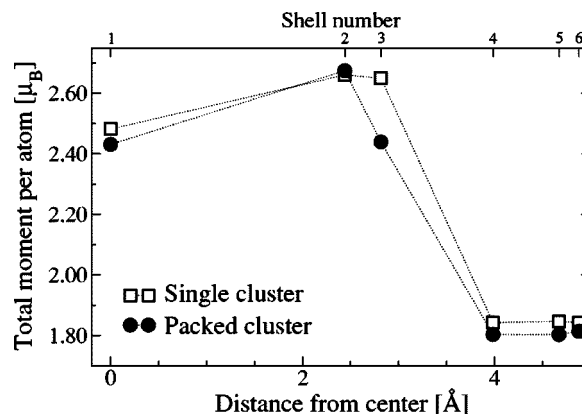


FIG. 8. Total magnetic moment per atom for each shell for single and packed Fe clusters. For the packed cluster, the Fe moments close to the Fe—Co interface decrease since the nearest-neighbor coordination is changed.

cell is shown in Fig. 8. The magnetic moments of the Fe atoms are smaller for the supercell system than for the impurity system, primarily for the atoms close to the interface with Co atoms. This is consistent with the magnetic enhancement being caused by the nearest-neighbor interaction since for the single cluster, the outmost Fe atom has four Co neighbors while the corresponding atom in the supercell have no Co nearest neighbors at all.

The average magnetic moment for this system is plotted in Fig. 6 and it is only $2.40\mu_B$ per atom, which is lower than the estimation from our simplified model, described above. Since the average moment for this close-packed structure of the Fe₁₅ clusters decreased significantly from the noninteracting cluster model, it is expected that the average moment would decrease for other cluster sizes as well. This indicates that, using theoretical spin and orbital moments for the clusters, it is unlikely to obtain saturation magnetizations exceeding the current limit of ~ 2.45 T for realistic systems of bcc Fe clusters embedded in bcc Co.

A better way to increase the magnetization density might be to embed Fe clusters not in Co but in materials that lie closer to the peak of the Slater-Pauling curve such as ordered (D0₃ or B₂) or disordered Fe—Co alloys. Such studies are underway.

IV. CONCLUSIONS

We have calculated spin and orbital moments for clusters of Fe atoms embedded in Co. The spin moments for the Fe

atoms are found to be sensitive to the local environment, where the presence of Co atoms as nearest neighbors increases the spin moment on the Fe atoms. We have compared our results with previous XMCD measurements and the total magnetic moments show good agreement with an error not exceeding 5%. For the orbital moments we observe a larger discrepancy, where our calculated values are close to the experimental bulk moment. The large measured orbital moments are probably due to structural relaxation effects in the clusters or due to difficulties in interpreting the experimental XMCD results.

By using a simple model without cluster-cluster interactions, we have estimated that high saturation magnetization can in principle be obtained by close packing small Fe clusters in a Co matrix. However, when taking cluster-cluster interactions into account, the magnetic moments decrease notably. This implies that the saturation magnetization for clusters of bcc Fe in a bcc Co matrix will be smaller than that for ordered alloys.

ACKNOWLEDGMENTS

This work was carried out with financial support from the Swedish Research Council (VR), the Foundation for Strategic Research (SSF), the Göran Gustafsson Foundation, and from Seagate Technology. We also acknowledge support from the Swedish National Super Computer facility (NSC).

*Electronic address: Anders.Bergman@fysik.uu.se

¹W. Eberhardt, Surf. Sci. **500**, 242 (2002).

²I. M. L. Billas, A. Chatelain, and W. A. de Heer, Science **265**, 1682 (1994).

³I. M. L. Billas, J. A. Becker, A. Chatelain, and W. A. de Heer, Phys. Rev. Lett. **71**, 4067 (1993).

⁴J. A. Franco, A. Vega, and F. Aguilera-Granja, Phys. Rev. B **60**, 434 (1999).

⁵T. Oda, A. Pasquarello, and R. Car, Phys. Rev. Lett. **80**, 3622 (1998).

⁶G. M. Pastor, J. Dorantes-Davila, S. Pick, and H. Dreysse, Phys. Rev. Lett. **75**, 326 (1995).

⁷M. Castro and D. R. Salahub, Phys. Rev. B **49**, 11842 (1994).

⁸O. Dieguez, M. M. G. Alemany, C. Rey, P. Ordejon, and L. J. Gallego, Phys. Rev. B **63**, 205407 (2001).

⁹A. Postnikov and P. Enter, Phase Transitions **77**, 149 (2004).

¹⁰C. Binns, Surf. Sci. Rep. **44**, 1 (2001).

¹¹J. Shen and J. Kirschner, Surf. Sci. **500**, 300 (2002).

¹²A. E. Berkowitz, J. R. Mitchell, M. J. Carey, A. P. Young, S. Zhang, F. E. Spada, F. T. Parker, A. Hutten, and G. Thomas, Phys. Rev. Lett. **68**, 3745 (1992).

¹³J. Q. Xiao, J. S. Jiang, and C. L. Chien, Phys. Rev. Lett. **68**, 3749 (1992).

¹⁴S. Mitani, H. Fujimori, K. Takanashi, K. Yakushiji, J. G. Ha, S. Takahashi, S. Maekawa, S. Ohnuma, N. Kobayashi, and T. Masumoto, J. Magn. Magn. Mater. **198–199**, 179 (1999).

¹⁵V. S. Stepanyuk, W. Hergert, P. Rennert, K. Wildberger, R. Zeller,

and P. H. Dederichs, Surf. Sci. **377–379**, 495 (1997).

¹⁶Ž. Šljivančanin and A. Pasquarello, Phys. Rev. Lett. **90**, 247202 (2003).

¹⁷B. Lazarovits, L. Szunyogh, and P. Weinberger, Phys. Rev. B **65**, 104441 (2002).

¹⁸I. Cabria, B. Nonas, R. Zeller, and P. H. Dederichs, Phys. Rev. B **65**, 054414 (2002).

¹⁹Y. Xie and J. A. Blackman, Phys. Rev. B **66**, 085410 (2002).

²⁰A. Vega, L. C. Balbas, J. Dorantes-Davila, and G. M. Pastor, Phys. Rev. B **50**, 3899 (1994).

²¹R. N. Nogueira and H. M. Petrilli, Phys. Rev. B **60**, 4120 (1999).

²²M. F. Collins and J. B. Forsyth, Philos. Mag. **8**, 401 (1963).

²³R. M. Bozorth, *Ferromagnetism* (Van Nostrand, New York, 1951).

²⁴S. H. Baker, C. Binns, K. W. Edmonds, M. J. Maher, S. C. Thornton, S. Louce, and S. S. Dhesi, J. Magn. Magn. Mater. **247**, 19 (2002).

²⁵C. Binns, K. W. Edmonds, S. H. Baker, S. C. Thornton, and M. D. Upward, Scr. Mater. **44**, 1303 (2001).

²⁶K. W. Edmonds, C. Binns, S. H. Baker, M. J. Maher, S. C. Thornton, O. Tjernberg, and N. B. Brookes, J. Magn. Magn. Mater. **220**, 25 (2000).

²⁷S. Frota-Pessoa, Phys. Rev. B **46**, 14570 (1992).

²⁸O. K. Andersen, O. Jepsen, and D. Glötzel, *Highlights of Condensed-Matter Theory* (North Holland, New York, 1985).

²⁹H. L. Skriver, *The LMTO Method* (Springer-Verlag, Berlin, 1984).

- ³⁰R. Haydock, *Solid State Physics* (Academic, New York, 1980), Vol. 35, p. 216.
- ³¹P. R. Peduto, S. Frota-Pessoa, and M. S. Methfessel, *Phys. Rev. B* **44**, 13283 (1991).
- ³²O. Eriksson, L. Bergqvist, E. Holmström, A. Bergman, O. LeBacq, S. Frota-Pessoa, B. Hjörvarsson, and L. Nordström, *J. Phys.: Condens. Matter* **15**, 599 (2003).
- ³³O. Eriksson, M. S. S. Brooks, and B. Johansson, *Phys. Rev. B* **41**, 7311(R) (1990).
- ³⁴H. Ebert, P. Strange, and B. Gyorffy, *J. Phys. F: Met. Phys.* **18**, L135 (1988).
- ³⁵O. Eriksson, B. Johansson, R. C. Albers, A. M Boring, and M. S. S. Brooks, *Phys. Rev. B* **42**, R2707 (1990).
- ³⁶N. Beer and D. Pettifor, *The Electronic Structure of Complex Systems* (Plenum Press, New York, 1984).
- ³⁷V. von Barth and L. Hedin, *J. Phys. Chem.* **5**, 1629 (1972).
- ³⁸A. Zangwill, *Physics at Surfaces* (Cambridge University Press, Cambridge, 1988).
- ³⁹P. Blomqvist, R. Wäppling, A. Broddefalk, P. Nordblad, S. G. E. te Velthuis, and G. P. Felcher, *J. Magn. Magn. Mater.* **248**, 75 (2002).
- ⁴⁰A. M. N. Niklasson, B. Johansson, and H. L. Skriver, *Phys. Rev. B* **59**, 6373 (1999).
- ⁴¹I. Turek, J. Kudrnovsky, V. Drchal, and P. Weinberger, *Phys. Rev. B* **49**, 3352 (1997).
- ⁴²I. A. Abrikosov, P. James, O. Eriksson, P. Söderlind, A. V. Ruban, H. L. Skriver, and B. Johansson, *Phys. Rev. B* **54**, 3380 (1996).
- ⁴³P. Mohn, *Magnetism in the Solid State* (Springer-Verlag, Berlin, 2003).
- ⁴⁴C. Binns, S. H. Baker, S. Louch, F. Sirotti, H. Cruguel, P. Prieto, S. C. Thornton, and J. D. Bellier, *Appl. Surf. Sci.* **226**, 249 (2004).